Dimensionally reduced SYM$_4$ at large-N: an intriguing Coulomb approximation

Daniele Dorigoni[a,b,c], Gabriele Veneziano[d,e] and Jacek Wosiek[f]

[a] *Scuola Normale Superiore, Piazza dei Cavalieri 7, 56126 Pisa, Italy*
[b] *Department of Physics "E.Fermi", Pisa University, Largo B.Pontecorvo 3, Ed.C, 56127 Pisa, Italy*
[c] *INFN, Sezione di Pisa, Largo B.Pontecorvo 3, Ed.C, 56127 Pisa, Italy*
[d] *Collège de France, 11 place M. Berthelot, 75005 Paris, France*
[e] *Theory Division, CERN, CH-1211 Geneva 23, Switzerland*
[f] *Smoluchowski Institute of Physics, Jagellonian University Reymonta 4, 30-059 Cracow, Poland*

Abstract

We consider the light-cone (LC) gauge and LC quantization of the dimensional reduction of super Yang Mills theory from four to two dimensions. After integrating out all unphysical degrees of freedom, the non-local LC Hamiltonian exhibits an explicit $\mathcal{N} = (2, 2)$ supersymmetry. A further SUSY-preserving compactification of LC-space on a torus of radius R, allows for a large-N numerical study where the smooth large-R limit of physical quantities can be checked. As a first step, we consider a simple, yet quite rich, "Coulomb approximation" that maintains an $\mathcal{N} = (1, 1)$ subgroup of the original supersymmetry and leads to a non-trivial generalization of 't Hooft's model with an arbitrary –but conserved– number of partons. We compute numerically the eigenvalues and eigenvectors both in momentum and in position space. Our results, so far limited to the sectors with 2, 3 and 4 partons, directly and quantitatively confirm a simple physical picture in terms of a string-like interaction with the expected tension among pairs of nearest-neighbours along the single-trace characterizing the large-N limit. Although broken by our approximation, traces of the full $\mathcal{N} = (2, 2)$ supersymmetry are still visible in the low-lying spectrum.

October 2010

1   Introduction

Supersymmetric (SUSY) gauge theories give us a useful playground where we can test and try to understand non-perturbative features of gauge-theories. On the other hand large-N expansions of various kinds [1, 2] provide further simplifications in the non-perturbative dynamics to the extent that suitable combinations of SUSY and large-N often result in models that can be (almost) fully understood analytically and/or numerically. A well known example of such a powerful mix is, of course, the AdS/CFT correspondence [3, 4].

Another application of the same set of ideas is the so-called planar equivalence [5, 6] between gauge theories with Dirac fermions in the antisymmetric (or symmetric) 2-index representation of $SU(N)$ and theories with Majorana fermions in the adjoint. Such a correspondence (which holds at large volume for a "common sector" in the two theories) could be physically relevant if $N = 3$ is "large-enough" since the former theories become, in that case, QCD-like. On the other hand, the adjoint-fermion theories become, in some cases, supersymmetric hence allowing to make predictions such as that of the quark condensate in QCD from the known value of the gluino condensate in $\mathcal{N} = 1$ super-Yang-Mills theory [7, 8].

Furthermore, $SU(N)$ gauge theories with $N_f \geq 1$ adjoint fermions appear to present another peculiar large-N virtue, volume independence [9, 10], according to which their properties at infinite volume are still captured if we consider them on a partially compactified space $\mathbb{R}^3 \times S^1$ with periodic boundary conditions both for the bosons and for the fermions. As the center symmetry appears to be unbroken in this case even at small volume [11], we can send the volume of the S^1 to zero and yet recover, at large-N, the large-volume physics (unlike the case of the well known Eguchi-Kawai reduction [12] for fundamental fermions). Combining planar equivalence and volume independence we may dream of calculating part of the spectrum of QCD (modulo $1/N$-corrections) by a small-volume calculation in a gauge theory with Majorana adjoint fermions.

Having in mind these motivations, we combine in this work large-N reduction and SUSY ideas by considering the well-known $\mathcal{N} = 1$ supersymmetric $SU(N)$ Yang-Mills (SYM) theory compactified to two dimensions. However, since the precise connection of this model with four-dimensional SYM theory is not yet clear [9], we should consider for the time being this model for its own sake as a two-dimensional (and, to our knowledge, so far unsolved) model.

We will be using a LC gauge and LC quantization [13], which has the advantage that all the unphysical degrees of freedom can be integrated out at the price of introducing Dirac brackets, a common procedure for constrained systems. The final outcome is a 2-dimensional $\mathcal{N} = (2,2)$ supersymmetric gauge theory on the light-cone. It appears to have an exact SUSY vacuum and a well-defined, normal-ordered, positive-semidefinite LC Hamiltonian that can be written as an anticommutator of supercharges. At large N this Hamiltonian acts on color-singlet physical states that can be written in terms of single-trace operators:

$$\text{Tr}\left(o_1(k_1)^\dagger ... o_n(k_n)^\dagger\right)|0\rangle$$

where the different $o_i^\dagger$ will represent either bosons or fermions with different light-cone

momenta $k_i > 0$.

The full Hamiltonian is still quite involved. In this paper, after having identified some "leading" terms which present potential Coulomb-like infrared singularities, we will define a natural Coulomb approximation to the full Hamiltonian. We show that, in this rather drastic approximation, the model becomes a partially (i.e. $\mathcal{N} = (1,1)$) supersymmetric generalization [14] of 't Hooft's model in two dimensions [15] with non-interacting sectors characterized by the number and species of partons they contain.

Some analytic results will be presented but most of the calculations will be numerical. This is done by discretizing the LC momenta [16] $k_i = n\epsilon$, thereby reducing the problem to the diagonalization of a large $M \times M$ hermitean matrix. We then prove that our discretization indeed converges to a continuum-limit once we take the $\epsilon \to 0$ ($M \to \infty$) limit.

The rest of the paper is organized as follows: in Section 2 we sketch the derivation of the LC two-dimensional theory starting from the SYM Lagrangian in four dimensions. We give the explicit expressions for the SUSY charges, light-cone momentum and Hamiltonian that satisfy the usual SUSY algebra. In Section 3 we introduce our Coulomb approximation and show how its apparent infrared divergences neatly cancel for colour-singlet states leaving behind the effects of a confining linear potential. In Section 4 we introduce a LC compactification of the two-dimensional theory as a devise to work with discrete values of the light-cone momenta. In Section 5 we give our analytic and numerical results for the 2, 3 and 4 partons sectors of the Coulomb Hamiltonian and discuss the left-over traces of the original supersymmetry. Finally, in Section 6, we give some conclusions and a short outlook.

2 Light-cone SYM$_4$ and its dimensional reduction

Our starting point is 4-dimensional $\mathcal{N} = 1$ super Yang-Mills (SYM) theory as defined by the Lagrangian [17]:

$$\mathcal{L} = -\frac{1}{4}F^a_{\mu\nu}F^{a\mu\nu} + i\lambda^{a\dagger}\bar{\sigma}^\mu D_\mu \lambda^a = \text{Tr}\left[-\frac{1}{2}F_{\mu\nu}F^{\mu\nu} + 2i\lambda^\dagger D_\mu \bar{\sigma}^\mu \lambda\right]. \tag{1}$$

The gauge group is $SU(N)$ and we have set to zero a possible θ-term since it can be rotated away in the absence of a gluino mass (i.e. as long as we do not break SUSY). We shall use the following conventions:

$$F^a_{\mu\nu} = \partial_\mu A^a_\nu - \partial_\nu A^a_\mu - gf^{abc}A^b_\mu A^c_\nu, \ D_\mu\lambda^a = \partial_\mu\lambda^a - gf^{abc}A^b_\mu\lambda^c,$$

$$A_\mu = A^a_\mu T^a_{fund}, \ F_{\mu\nu} = F^a_{\mu\nu}T^a_{fund} = \partial_\mu A_\nu - \partial_\nu A_\mu + ig[A_\mu, A_\nu], D_\mu\lambda = \ \partial_\mu\lambda + ig[A_\mu, \lambda].$$

We now introduce LC coordinates $x^\pm = \frac{x^0 \pm x^3}{\sqrt{2}}$ and fix the LC gauge $A_- = 0$. As a result we can rewrite (1) as:

$$\mathcal{L} = \text{Tr}\left[(\partial_- A_+)^2 + 2(\partial_- A(\partial_+ A^\dagger - \bar{D}A_+) + \partial_- A^\dagger(\partial_+ A - DA_+)) + \right.$$

$$\left. (\bar{D}A - DA^\dagger - ig[A^\dagger, A])^2 + 2\sqrt{2}i\lambda^\dagger \begin{pmatrix} \partial_- & -\bar{D} \\ -D & D_+ \end{pmatrix}\lambda\right], \tag{2}$$

2

where we have introduced $A = (A_1 + iA_2)/\sqrt{2}$, $A^\dagger = (A_1 - iA_2)/\sqrt{2}$, $D_{1+i2} \equiv \sqrt{2}D = \sqrt{2}(\partial + ig[A, \times])$ and its hermitean conjugate $D_{1-i2} \equiv \sqrt{2}\bar{D} = \sqrt{2}(\bar{\partial} + ig[A^\dagger, \times])$.

The fields A_+ and λ_1 become non-dynamical (in the sense that their equations of motion do not involve derivatives with respect to the lightcone time x^+) and can be integrated out. Furthermore, we can consider the reduction of the theory to $D = 2$ by discarding all dependencies on $x^\perp$ and hence by setting to zero ∂ and $\bar{\partial}$. As a result the Lagrangian under consideration becomes:

$$\mathcal{L}^r_{io} = \text{Tr}\left[J^+_r \frac{1}{\partial^2_-} J^+_r + 2(\partial_- A\partial_+ A^\dagger + \partial_+ A\partial_- A^\dagger) - g^2[A, A^\dagger]^2 + \right.$$
$$\left. + 2\sqrt{2}i(\lambda^*_2\partial_+\lambda_2 - g^2[A, \lambda^*_2]\frac{1}{\partial_-}[A^\dagger, \lambda_2]) \right], \tag{3}$$

where the subscript io means that we have integrated out the non-dynamical fields and the superscript r tells us that this is now a theory in 2-dimensions $x^\pm$. The (reduced) current J^+_r turns out to be:

$$J^+_r = ig[A^\dagger, \partial_- A] + ig[A, \partial_- A^\dagger] + \sqrt{2}\,g\{\lambda^*_2, \lambda_2\}. \tag{4}$$

To obtain the Hamiltonian from (3) we have simply to perform a Legendre transform:

$$H^r_{io} = \text{Tr}\left[-J^+_r \frac{1}{\partial^2_-} J^+_r + g^2\,[A, A^\dagger]^2 + 2\sqrt{2}i\,g^2[A, \lambda^*_2]\frac{1}{\partial_-}[A^\dagger, \lambda_2] \right], \tag{5}$$

We have to keep in mind, however, that the right commutation relations are those obtained from Dirac –rather than Poisson– brackets: only then the constraints implicitly used will be preserved by the LC-time evolution generated by H^r_{io}. This leads to the following quantization of the dynamical fields A and λ_2 in terms of creation/annihilation operators with a Fock vacuum $|0\rangle$[1]:

$$A^a(0, x^-) = \int_0^\infty \frac{dk^+}{\sqrt{2\pi}\sqrt{2k^+}}\left[a^a(k^+)e^{-ik^+x^-} + b^{\dagger a}(k^+)e^{+ik^+x^-} \right],$$
$$\lambda^a_2(0, x^-) = \int_0^\infty \frac{dk^+}{2^{1/4}\sqrt{2\pi}}\left[f^a(k^+)e^{-ik^+x^-} + g^{\dagger a}(k^+)e^{+ik^+x^-} \right],$$
$$[a^a(k^+), a^{\dagger b}(k'^+)] = [b^a, b^{\dagger b}] = \{f^a, f^{\dagger b}\} = \{g^a, g^{\dagger b}\} = \delta(k^+ - k'^+)\delta^{ab}, \tag{6}$$

and of course all other (anti-)commutators vanish. Note that in order to obtain precisely the Dirac commutation relations we have to take our LC momenta k^+ to be positive.

The theory thus obtained can be seen as the $\mathcal{N} = (2, 2)$ two-dimensional supersymmetric theory that follows from the dimensional reduction of $\mathcal{N} = 1$ super Yang-Mills on

---

[1]We have assumed a vanishing VEV for the scalar field although, even in $D = 2$, we expect the classical moduli space to be preserved since tunneling should be suppressed in the large-N limit. If so the spectrum will depend on the particular point chosen in moduli space. One of us (GV) is grateful to A. Armoni and A. Schwimmer for a discussion concerning this point.

$\mathbb{R}^2 \times T^2$. Note, however, that due to the non-susy invariance of the gauge fixing the transformations generated by the supercharges through Dirac brackets will not be the usual one but will have to be supplemented by an additional gauge transformation needed to restore the gauge constraint $A_- = 0$. This is already true before compactification (where one gets $\mathcal{N} = 1$ SUSY in $D = 4$) and keeps working after compactifying on $\mathbb{R}^2 \times T^2$ i.e. if we keep only the zero-modes (hence setting $\partial/\partial x^\perp = 0$). A straightforward calculation leads to the following form for the supersymmetric charges, momentum and Hamiltonian operators:

$$
\begin{aligned}
Q_2 &= \int dx^- \, 2\sqrt{2}\partial_- A^a \lambda_2^{*a} \\
&= 2^{3/4} \int_0^\infty dk_1 dk_2 \, \sqrt{k_1}\delta(.) \left(b_{k_1}^{a\dagger} g_{k_2}^a - a_{k_1}^a f_{k_2}^{a\dagger} \right), \quad (7)
\end{aligned}
$$

$$
\begin{aligned}
P_- &= \frac{1}{2\sqrt{2}}\{Q_2, \bar{Q}_{\dot{2}}\} = \int dx^- \, (2\partial_- A^{\dagger a}\partial_- A^a + i\sqrt{2}\lambda_2^{*a}\partial_-\lambda_2^a) \\
&= \int_0^\infty dk \, k \left[a_k^{\dagger a} a_k^a + b_k^{\dagger a} b_k^a + f_k^{\dagger a} f_k^a + g_k^{\dagger a} g_k^a \right], \quad (8)
\end{aligned}
$$

$$
\begin{aligned}
Q_1 &= \int dx^- (-2\sqrt{2}g f^{abc} A^{\dagger a}\partial_- A^b + 2ig f^{abc}\lambda_2^a \lambda_2^{*b})\frac{1}{\partial_-}\lambda_2^{*c} \\
&= \frac{g}{2^{1/4}\sqrt{\pi}} \int_0^\infty dk_1 dk_2 dk_3 \, \delta(.) f^{abc} \left[\frac{\sqrt{k_2}}{k_3\sqrt{k_1}} \left(a_{k_1}^{a\dagger} a_{k_2}^b g_{k_3}^c - a_{k_1}^{a\dagger} a_{k_2}^b f_{k_3}^{c\dagger} \right. \right. \\
&\quad \left. + b_{k_1}^a b_{k_2}^{b\dagger} f_{k_3}^{c\dagger} - b_{k_1}^a b_{k_2}^{b\dagger} g_{k_3}^c \right) + \frac{\sqrt{k_1}}{k_3\sqrt{k_2}} \left(b_{k_1}^{a\dagger} a_{k_2}^{b\dagger} g_{k_3}^c + a_{k_1}^a b_{k_2}^b f_{k_3}^{c\dagger} \right) \\
&\quad \left. + \frac{(k_3 + k_2)}{2k_3 k_2} \left(g_{k_1}^{a\dagger} g_{k_2}^b g_{k_3}^c - f_{k_1}^a f_{k_2}^{b\dagger} f_{k_3}^{c\dagger} \right) + \frac{(k_2 - k_3)}{k_3 k_2} \left(f_{k_1}^a f_{k_2}^{b\dagger} g_{k_3}^c + g_{k_1}^{a\dagger} f_{k_2}^{b\dagger} g_{k_3}^c \right) \right] \quad (9)
\end{aligned}
$$

$$
P_+ = \frac{1}{2\sqrt{2}}\{Q_1, \bar{Q}_{\dot{1}}\} = \int dx^- H_{io}^r, \quad (10)
$$

where $\delta(.)$ is a shorthand notation for $\delta(\pm k_1 \pm ...)$ where the sign plus is for creation operator while the minus sign otherwise. We did not report here the explicit momentum space version for P_+ since, as the reader may guess from the rather involved expression for Q_1, its expression is quite long and not particularly illuminating. A lengthy calculation shows that the above charges satisfy the $\mathcal{N} = (2, 2)$ SUSY algebra:

$$
\begin{aligned}
\{Q_1, \bar{Q}_1\} &= 2\sqrt{2}P_+ = 2\sqrt{2}H_{io}^r, \\
\{Q_2, \bar{Q}_2\} &= 2\sqrt{2}P_-, \quad (11)
\end{aligned}
$$

with all other anticommutators vanishing identically.

As we will see in the following sections one can compactify also the x^- direction and replace all the integrals $\int_0^\infty dk$ with sums over positive integers $\sum_{n=1}^\infty$, the key point is precisely that all LC momenta have to be greater than zero, so we can actually rewrite $\int_0^\infty dk = \int_{-\infty}^{+\infty} dk \, \theta(k)$. We note, incidentally that in [18] it was claimed that the discretized

version of the supercharges does not satisfy the susy algebra. We claim instead that everything works fine provided an appropriate care is used in performing the discretization and in defining the (anti)commutators; particular attention is needed when, by momentum conservation, an intermediate parton gets a vanishing momentum: by adopting a careful prescription for the ensuing $\theta(0)$ we can fully maintain supersymmetry.

2.1 General properties of the reduced theory

Let us discuss some exact features of the complete SUSY charges and Hamiltonian. The Hamiltonian conserves parton number parity $(-1)^p$ (actually changes p by $0, \pm 2$) and therefore splits into two sectors with even and odd number of partons. On the other hand the charges $Q_2, Q_2^\dagger$ preserve p while $Q_1, Q_1^\dagger$ change p by ± 1.

Besides P_- there is another conserved quantity, J_z, which is what remains of the original helicity of the 4-D theory. The four partons a, b, f, g have $J_z = +1, -1, +1/2, -1/2$ respectively and the hamiltonian is block-diagonal with subspaces of fixed total J_z while $Q_1, Q_2^\dagger$ change J_z by $+1$ and $Q_2, Q_1^\dagger$ by -1.

Consider for instance a supermultiplet containing a $J_z = 0$ boson $|x\rangle$ of non-vanishing mass. Since its p_+ and p_- are both non-vanishing this state can be at most annihilated by one out of $Q_1, Q_1^\dagger$ and similarly by one out of $Q_2, Q_2^\dagger$. Acting on $|x\rangle$ in all possible ways we see that we generate a supermultiplet containing two bosons with opposite parton number parity and two fermions with opposite parton parity. However CPT invariance requires the existence of a similar multiplet of antiparticles and we end up with 4 bosons and 4 fermions as the minimal size of a massive supermultiplet[2].

As an example, consider the anomaly (or Konishi) supermultiplet $S \equiv \epsilon^{\alpha\beta} W_\alpha W_\beta$. Its lowest component is the gaugino bilinear $\epsilon^{\alpha\beta}\lambda_\alpha\lambda_\beta$ which is just proportional to $\lambda_1\lambda_2$. Since in our setup λ_1 is expressed in terms of λ_2 and $\bar{A}$ we see that, at first order, $S|0\rangle$ gives a state of the type $|gga\rangle$. Such a state is clearly annihilated by $\bar{Q}_2$ (but not by Q_2) and one can consistently assume that it is annihilated by $\bar{Q}_1$ (and not by Q_1), which mimics exactly the situation in $D = 4$. Acting on $|gga\rangle$ with Q_1, Q_2 and $[Q_1, Q_2]$ (the anticommutator being zero), we generate two fermionic states (whose lowest p components look like $|ga\rangle$ and a combination of $|ggf\rangle$ and $|gab\rangle$) and one more scalar (a combination of $|ab\rangle$ and $|fg\rangle$ with additional $p > 2$ components). This gives a total of 2 bosons and 2 fermions to which we have to add a similar set of states starting from $\bar{S}|0\rangle \sim |ffb\rangle$.

As we shall see, our approximation to the full Hamiltonian breaks SUSY to an $\mathcal{N} = (1, 1)$ subgroup of the full $\mathcal{N} = (2, 2)$ and therefore to the breaking of some degeneracies. Nonetheless, an approximate full degeneracy will be seen to remain even in our very simple system with Coulomb interactions only.

---

[2]This is only apparently in contrast with the counting of states in $D = 4$ but it is not since, in $D = 2$ there is a further doubling of states due to to the distinction between left- and right-movers [19].

3 Cancellation of leading infrared divergences and a Coulomb approximation

In our LC quantization the supercharge Q_2 and the momentum P_- are like in a free theory and thus trivial. By contrast, the supercharge Q_1 and the "Hamiltonian" P_+ are highly not trivial: non-linear and even non-local. Let us discuss some of their properties before making any approximation. From (9) we see that every term appearing in Q_1 is trilinear in creation/annihilation operators. Furthermore, since the LC momenta are all positive, momentum conservation implies the absence of pure creation or pure annihilation terms. Thus Q_1 connects states with opposite parton-number parity. The LC Hamiltonian, $\{Q_1, \bar{Q}_1\}$, will have either quadratic terms (with one creation and one annihilation operator), or quartic terms. Since no pure destruction or pure creation operators appear in H_{io}^r the Fock vacuum is annihilated both by the SUSY charges and by the Hamiltonian and is an exact zero-energy ground state. The quartic terms induce either $2 \to 2$ or $1 \to 3, 3 \to 1$ transitions and thus conserve $(-1)^p$.

The full Hamiltonian exhibits, at least superficially, both linear and logarithmic infrared (IR) divergences when some momenta (or combinations thereof) go to zero. The logarithmic divergences, that resemble those of the $4D$ theory, presumably need a Block-Nordsieck treatment that we plan to implement (analytically and/or numerically) in a forthcoming paper. The linear, Coulomb-like divergences are instead neatly cancelled for colour-singlet states as we shall now argue. Nevertheless, the finite effects they leave behind are expected to dominate the Hamiltonian at large distances.

In order to illustrate this feature we introduce a rather crude "Coulomb approximation", in which we keep only the linearly-divergent terms in the Hamiltonian in their minimal form of $1/q^2$ poles. Such IR singularities only appear in the quadratic terms (which are necessarily diagonal) and in the elastic $2 \to 2$ scattering terms. In the above-mentioned approximation the former take the simplified form:

$$H_C^{quad} = \frac{\lambda}{\pi} \sum_A \mathrm{Tr} \int_0^\infty dk \int_0^k \frac{dq}{q^2} A_k^\dagger A_k \;\; ; \;\; \lambda \equiv g^2 N_c \;\; , \tag{12}$$

where A stands for any one of the four parton species. Similarly the elastic quartic terms can be simplified as:

$$H_C^{elastic} = -\sum_{A,B} \frac{g^2}{2\pi} \int_0^\infty dp_1 dp_2 \left[\int_0^{p_1} \frac{dq}{q^2} \mathrm{Tr}(A_{p_1}^\dagger B_{p_2}^\dagger B_{p_2+q} A_{p_1-q}) + \right.$$
$$\left. + \int_0^{p_2} \frac{dq}{q^2} \mathrm{Tr}(A_{p_1}^\dagger B_{p_2}^\dagger B_{p_2-q} A_{p_1+q}) \right] \;\; , \tag{13}$$

where A, B stand for any one of the four parton species. Note that these elastic terms neither change the number of partons nor their species. For this reason we can restrict ourselves to subspaces of the entire Hilbert space of states with a given set (i.e. number

and species) of partons and fixed total momentum $P_-(\equiv P$ below). Furthermore, as discussed in Section 1, the 't Hooft limit, $N \to \infty$ with λ fixed, selects single trace states as the only relevant ones (transitions with multi-trace states being $1/N$-suppressed).

In conclusion, we can diagonalize H_C by splitting the total Hilbert space generated by a generic linear superposition of single-trace states into subspaces of definite total momentum P and definite parton number p:

$$
\mathcal{H}_P^p = \left\{ |s\rangle = \mathrm{Tr}\left(o_1^\dagger(k_1) o_2^\dagger(k_2) ... o_{p-1}^\dagger(k_{p-1}) o_p^\dagger(P - \sum_{i=1}^{p-1} k_i) \right) |0\rangle \right\}, \qquad (14)
$$

where $o_i^\dagger$ can be any of our creation operators and all the momenta k_i satisfy $0 < k_i < P$ for $i = 1, ..., p$ and we define $k_p = P - \sum_{i=1}^{p-1} k_i$. Starting with section 5 we will study in detail, both analytically and numerically, the eigenvalues and eigenvectors of H_C restricted to $\mathcal{H}_P^2$, $\mathcal{H}_P^3$ and $\mathcal{H}_P^4$. For the numerical approach it will be convenient to discretize the LC momenta by compactifying the coordinate x^-. This will be discussed in the next section.

Before turning to actual calculations let us give a general argument for the cancellation of the Coulomb divergences for a general state of the form (14). Let us take an arbitrary pair of neighbour partons in (14) and consider four distinct contributions to their mutual and self-interaction. The self interactions come from the quadratic terms (12) for each one of the neighbour partons. However, in order to keep the book-keeping right, we attribute half of the quadratic term acting on each parton to its interaction with the left neighbour and half to the one with its right neighbour. The book-keeping is easier for the quartic Hamiltonian where one just keeps the terms corresponding to the exchange of quanta between the two selected partons (there are two such contributions, in general, depending on which of the two partons gains energy in the process).

When these four contributions are added one finds, for each pair of neighbours, the following result:

$$
H_C^{A-B} \varphi(\ldots p_A, p_B, \ldots) = \frac{\lambda}{2\pi} \int_{-p_B+\epsilon}^{p_A-\epsilon} dq \frac{\varphi(\ldots p_A, p_B, \ldots) - \varphi(\ldots p_A - q, p_B + q, \ldots)}{q^2},
$$
$$(15)$$

where $A - B$ stand for a pair of neighbours and $\varphi(p_1, ..., p_N)$ is the wavefunction in momentum space of the particular chosen state. The total Hamiltonian is given then by a sum over A and B. We see that the numerator on the r.h.s. vanishes at $q = 0$. If we take a smooth linear superposition of parton-momentum eigenstates, the numerator will vanish quadratically in q thus completely removing the singularity.

As a physical example of such a smooth superposition let us consider two partons displaced by some $\Delta x \equiv \Delta x^-$ in LC space. The momentum wavefunctions will combine to give an $e^{iq\Delta x}$ for the second term in the numerator so that, for each pair:

$$
H_C^{A-B} \simeq \frac{\lambda}{2\pi} \int_{-p_B}^{p_A} dq \frac{(1 - cos(q\Delta x))}{q^2} \simeq \frac{\lambda}{\pi} \int_{-\infty}^{\infty} dq \frac{sin^2(q\Delta x/2)}{q^2} = \frac{\lambda}{2}|\Delta x|, \qquad (16)
$$

at large separations. We have just discovered that the Coulomb Hamiltonian, acting on a single trace state, produces an energy proportional to the sum of the $|\Delta x_{ij}^-|$ distances for

each pair of neighbouring partons. The constant of proportionality turns out to be just $\frac{\lambda}{2}$ i.e. nothing but the $2D$ string tension for sources in the fundamental representation [20, 21][3]. This is as it should be, since each parton behaves, vis-a-vis of its neighbours, like a parton in the fundamental representation. Its belonging to the adjoint representation reveals itself in the fact that it has *two* neighbours. For a two parton system this just produces the well known factor two difference between adjoint and fundamental tension in the large-N limit. A numerical verification of this analytic argument will be given in Sect. 6.

4   Light-cone compactification

We now further compactify, for computational convenience, the x^- direction on a circle of radius R (with periodic boundary conditions). As a consequence, the p_- momenta are quantized[4]:

$$p_- = n\frac{\hbar}{R} \equiv n\epsilon \, , \, n = 0, 1, \ldots \tag{17}$$

The total conserved momentum is taken to be

$$P_- \equiv P = K\frac{\hbar}{R} \equiv K\epsilon \tag{18}$$

and we shall be interested in the decompactification limit $R \to \infty$ ($\epsilon \to 0$). In order to keep P fixed this also means $K \to \infty$. Since in LC quantization all momenta are positive, P effectively plays the role of an ultraviolet cut off Λ_{UV}. In other words, in eq. (17), $n \le K$. If we also take out the zero mode ($n = 0$ in (17)), $\epsilon \equiv \hbar/R$ plays instead the role of an IR cutoff and $K = \frac{\Lambda_{UV}}{\Lambda_{IR}}$. The picture is similar to that of a (2-dimensional) lattice gauge theory in Hamiltonian formalism (continuous time and discretized space) with a lattice spacing given by $a = 2\pi\hbar/P = L/K$ and a total of K lattice points to cover a large circle of circumference $L = 2\pi R = Ka$.

According to the LC quantization philosophy, P_+ plays the role of the Hamiltonian and the Lorentz-invariant eigenvalue equation reads:

$$M^2|s\rangle = 2P_+P_-|s\rangle = 2PP_+|s\rangle = 2K\epsilon P_+|s\rangle \tag{19}$$

The eigenvalues (and eigenvectors) of this operator should have a finite limit as $K \to \infty$. We have found it convenient to work in units in which $\epsilon = 1$ (integer parton momenta). In that case the operator KP_+ should approach a finite limit as $K \to \infty$. More physically we could have chosen units in which $a = 1$ and momenta are quantized in units of $2\pi/K$. One can easily check that the limit $K \to \infty$ provides in both cases the same spectrum for M^2.

---

[3]This can be generalized to finite N with $C_F \equiv (N^2 - 1)/2N$ replacing $N/2$ (private communication by G. C. Rossi).

[4]In this section we shall keep Planck's constant explicit in order to illustrate the emergence of a quantum-mechanical string.
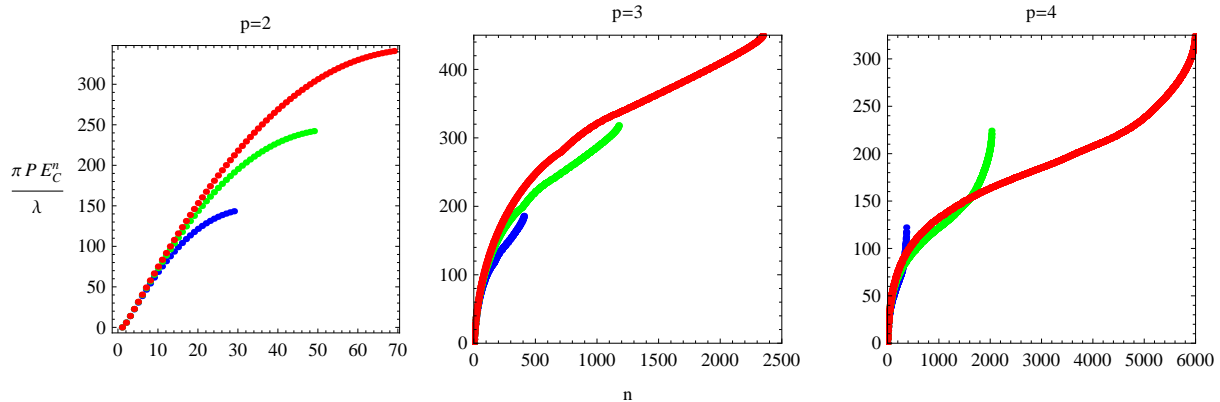
Figure 1: Cutoff dependence of the eigenvalues of H_C in the three lowest multiplicity sectors. The size of the H_C matrix grows with the resolution parameter K and can be read from the range covered on the horizontal axis, $K = 30, 50, 70$ for $p = 2, 3$, and $K = 15, 25, 35$ for $p = 4$.

We expect to find finite-size effects at finite K. Because of periodicity the maximal x^- distance is $Ka/2$ and therefore only states whose wavefunction is concentrated in regions much smaller than $Ka/2$ are expected to have already reached an asymptotic limit at some given K. We will see later that this is exactly what happens numerically, but let us anticipate the presentation of some of the results we will find for $p = 2$. Once we have discretized the momenta in units of $\epsilon \equiv 1$, the M^2 operator becomes an $(K-1) \times (K-1)$ matrix whose low eigenvalues converge fast to some finite values while increasing K. This can be seen in Fig. 1 (to be discussed in detail in Section 6) which illustrates what happens for $K = 30, 50$ and 70. This is equivalent to discretizing states with a fixed total momentum $P = 1$ by subsequently taking $\epsilon = 1/30, 1/50$ and $1/70$, We see a neat

9

convergence of the lowest eigenvalues towards a smooth (and almost linear) spectrum.

Referring still to the two-parton sector, we shall also find that the eigenvectors exhibit a sharp localization in position (i.e. x^-) space, or, more precisely, in the distance Δx^- between the two partons. The average distance appears to be quantized:

$$\langle \Delta x^- \rangle_n = c_n \frac{L}{K} = 2\pi c_n \frac{\hbar}{P_-} \quad , \quad n = 1, 2, \ldots K - 1 , \tag{20}$$

where the c_n are a sequence of numbers going from a number of $O(1)$ to a number of $O(K/2)$ in steps of $O(1)$. The ordering coincides with that of the energy eigenvalues. In other words, the average distance is of the order of $a = 2\pi\hbar/P_-$ for the lightest states and grows up to the maximal allowed physical distance for the heaviest eigenstates. As we increase K, the low-lying states stabilize while the heavy ones change and stabilize only at higher values of K (i.e. when Δx^- is well within the compact circle). The spread in Δx^- is $O(a)$ for all the states (this is the above-mentioned position-space localization).

The low-lying eigenvalues of P_+ behave like P_-^{-1} for large P_- and, indeed, one finds (c.f. Fig.9) an approximate linear relation between energy and average distance:

$$P_+^{(n)} \simeq \lambda \langle \Delta x^- \rangle_n \tag{21}$$

where λ is 't Hooft's coupling normalized in such a way that it corresponds to a classical tension. This means that an appealing string picture emerges whereby energies are proportional to the string tension λ. This result, however, is Lorentz-frame dependent. In order to find a Lorentz invariant result we compute the mass eigenvalues:

$$M_n^2 = 2P_- P_+^{(n)} \simeq 2\lambda P_- \langle \Delta x^- \rangle_n = 4\pi\hbar\lambda c_n = \lambda M_n \langle \Delta x^{cm} \rangle_n \tag{22}$$

where we have used first (20) and, for the last step, an n-dependent Lorentz transformation with boost $\sqrt{2}P_-/M_n$ in order to go to the nth state rest frame. Thus we finally obtain:

$$\langle \Delta x^{cm} \rangle_n = \sqrt{4\pi c_n} l_s \quad , \quad M_n \simeq \lambda \langle \Delta x^{cm} \rangle_n = \sqrt{4\pi c_n} M_s \tag{23}$$

in terms of the string length and mass scales: $l_s = \sqrt{\hbar/\lambda}$, $M_s \equiv \sqrt{\hbar\lambda}$. This is in perfect agreement with expectations[20, 21] once we realize that, for $p = 2$, the sum over neighbour-parton distances is $2\Delta x$.

5   Bases and matrix elements at large N_c

Below we quote a few explicit expressions for matrix elements of the discretized (and rescaled) Hamiltonian h_C defined by:

$$H_C = \frac{\lambda}{\pi} \frac{K}{P} h_C. \tag{24}$$

The mode expansion of h_C in terms of the discretized creation and annihilation operators

$$A_m = \frac{1}{\sqrt{R}} A_{m\epsilon} \tag{25}$$

is the same as in (13,12) with all momenta $p \to m$ and integrals $\int dp \to \sum_m$.

There are four kinds (species) of partons in our model: two bosons and two fermions with the corresponding annihilation operators denoted by a, b, f, g. The detailed construction of the planar bases in each multiplicity sector differs slightly depending on the particular choice of parton species involved and the same applies to the matrix elements of h_C (12,13).

5.1   Two different partons

At given resolution K the states belonging to the discretised version of $\mathcal{H}_K^2$ are labeled by one integer:

$$|n\rangle = Tr[A^\dagger{}_n B^\dagger{}_{K-n}]|0\rangle, \quad n = 1, ..., K - 1, \tag{26}$$

where $A, B = a, b, f, g$. The large N rules, developed e.g. in [22], give

$$\langle n|h_C|n'\rangle = \delta_{n,n'} \left(C(n) + C(K - n)\right) - (1 - \delta_{n,n'})\frac{1}{2(n - n')^2}$$

$$- (1 - \delta_{K-n,K-n'})\frac{1}{2(n - n')^2}, \tag{27}$$

$$C(n) = \sum_{q=1}^{n-1} \frac{1}{q^2}.$$

5.2   Two identical partons

In this case, due to the cyclic symmetry $n \to K - n$, only half of the states from above, is linearly independent. The matrix elements can be neatly expressed by (anti)symmetrized ones from the previous case

$$\langle n|h_C|n'\rangle_{id} = \langle n|h_C|n'\rangle_{dif} \pm \langle K - n|h_C|n'\rangle_{dif}, \quad n = 1, ...\frac{K - 1}{2}, \; K \, odd, \tag{28}$$

where the suffix id stands for identical partons and the suffix dif for different partons while the $+$ sign is for identical bosons and the $-$ for fermions. The union of the two (bosonic and fermionic) spectra for identical partons will reconstruct the complete spectrum obtained from eq.(27).

5.3   Three different partons

We consider now states composed by three different partons (taken as abf). These are labeled by two integers:

$$|n, m\rangle = Tr[a_n^\dagger b_m^\dagger f_{K-n-m}^\dagger]|0\rangle, \quad 1 \le n \le K - 2, \; 1 \le m \le K - n - 1 \tag{29}$$

11

and the matrix elements of Eq. (12,13) read:

$$
\begin{aligned}
\langle m, n | h_C | m', n' \rangle =& \delta_{m,m'} \delta_{n,n'} (C(m) + C(n) + C(K - m - n)) \\
& - \delta_{m,m'} (1 - \delta_{n,n'})/2(n - n')^2 \\
& - \delta_{n,n'} (1 - \delta_{m,m'})/2(m - m')^2 \\
& - \delta_{m+n,m'+n'} (1 - \delta_{m,m'})/2(m - m')^2 \,.
\end{aligned}
\tag{30}
$$

In the case of states with just two parton species (e.g. aaf) h_C has the same matrix elements. The Hilbert space is however twice as small since cyclic and anticyclic permutations correspond to the same state. On the other hand the bigger Hilbert space for three different species splits into two separate sectors, since states corresponding to above cyclic and anticyclic permutation do not interact in the planar limit.

5.4 Three identical partons

With a trick similar to the two parton case one can exploit the cyclic symmetry and express matrix elements in terms of those for three different partons

$$
\begin{aligned}
\langle n, m | h_C | n', m' \rangle_{id} =& \langle n, m | h_C | n', m' \rangle_{dif} + \langle m, K - n - m | h_C | n', m' \rangle_{dif} + \\
& + \langle K - n - m, n | h_C | n', m' \rangle_{dif} \,.
\end{aligned}
\tag{31}
$$

This time there is no difference between bosonic and fermionic sectors since $\mathbb{Z}_3$ shifts involve an even number of fermionic transpositions.

5.5 Four different partons, the *abfg* sector

.

The planar basis is now parametrized by three integers

$$
\begin{aligned}
|n, m, o\rangle =& Tr[a_n^\dagger b_m^\dagger f_o^\dagger g_{K-n-m-o}^\dagger]|0\rangle \,, \\
& 1 \leq n \leq K - 3 \,, \quad 1 \leq m \leq K - n - 2 \,, \quad 1 \leq o \leq K - m - n - 1 \,,
\end{aligned}
$$

and matrix elements of Eq. (12,13) read

$$
\begin{aligned}
\langle m, n, o | h_C | m', n', o' \rangle =& \delta_{m,m'} \delta_{n,n'} \delta_{o,o'} (C(m) + C(n) + C(o) + C(K - m - n - o)) \\
& - \delta_{m,m'} \delta_{n,n'} (1 - \delta_{o,o'})/2(o - o')^2 \\
& - \delta_{n,n'} \delta_{o,o'} (1 - \delta_{m,m'})/2(m - m')^2 \\
& - \delta_{o,o'} \delta_{m+n+o,m'+n'+o'} (1 - \delta_{n,n'})/2(n - n')^2 \\
& - \delta_{m+n+o,m'+n'+o'} \delta_{m,m'} (1 - \delta_{o,o'})/2(o - o')^2 \,.
\end{aligned}
\tag{32}
$$

Generalization to higher parton multiplicities is pretty straightforward.

6 Results

We turn now to discuss quantitative solutions obtained, mainly numerically, with the aid of Mathematica. The crude Coulomb approximation introduced above is not only the lowest approximation for the full set of the complete coupled LC eigenequations but, at the same time, it defines a natural generalization of 't Hooft equation to many-body sectors. Rather than concentrate on separate parton multiplicities, p, we shall focus on a few physical issues and compare results for different multiplicities. Until now only the first three nontrivial sectors, i.e. $p = 2, 3, 4$ have been looked upon. Obviously, further increase of p is technically more challenging, however it is feasible, if such a need arises, by employing more dedicated methods and algorithms.

6.1 K dependence vs. $K = \infty$ limit

Figure 1 summarizes the cutoff dependence of spectra of H_C for different multiplicities. As expected, lower states converge faster, however one should remember that at the high end of the spectrum new states appear for each K. Since K controls the length $L = 2\pi K/P$ of our torus, the highest state, for example, will never converge because it is a new state with higher and higher energy as we increase K.

The eigenenergies of PH_C (that is $M_n^2/2$) are displayed as a function of a single index n which labels consecutively ordered eigenvalues. Only for the two parton case n is directly related with a single physical observable (see below). For more partons, n is effectively composed of more quantum numbers related to other, yet unknown, quantities conserved in a particular many body sector. As a consequence, the $p = 2$ dependence is nicely linear, at large K, while the limiting curves for higher p are more complicated. They reflect the above degeneracy with more and more states below a fixed energy as we increase p. In fact one can read the spectral density of states dN/dE directly from the figure. It grows with E at intermediate energies, the growth becoming more and more rapid as we increase p. However at the highest end of the spectrum the density saturates revealing some sort of blocking related to periodicity.

Let us now look for the cutoff dependence of the lowest levels in more detail. Figure 2 shows the first few eigenenergies in the boson-boson and fermion-fermion, $p = 2$, sectors as a function of $1/K$. Evidently dependence on K is very weak and the extrapolation to the continuum momentum limit is straightforward. In fact, in this limit the LC eigenequations are nothing but 't Hooft equations with adjoint charges. Hence the limiting values can be obtained by solving directly these equations. They are also displayed in Figure 2, providing a rather satisfactory cross check of the whole approach.

Finally we comment on the difference between bound states made of fermionic and/or bosonic identical partons. Since H_C is invariant under the reflection $m \leftrightarrow K - m$, the non-degenerate eigenstates have definite parity. This is the case in the two parton sector. Moreover, the $\mathbb{Z}_2$ symmetry of planar states together with the "flavour" independence allows to identify the even and odd solutions as identical boson-boson and identical fermion-fermion bound states. In the $K = \infty$ case, we have generated corresponding eigenstates
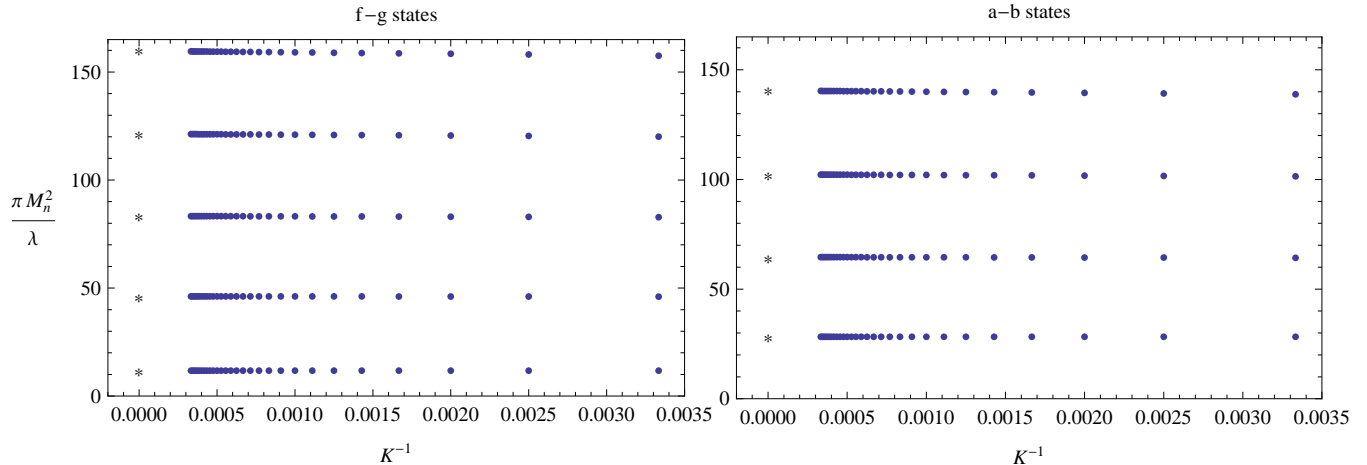
Figure 2: Convergence of the lowest energy levels with the cutoff ($100 \leq K \leq 3000$) and comparison between the even (identical boson-boson) and odd (identical fermion-fermion) solutions. Stars represent direct solutions of the 't Hooft equations for continuous momenta ($K = \infty$).

by employing bases with the required symmetry.

As usual, the lowest state is symmetric. It's wave function is constant in the parton momentum, k, with exactly zero eigenvalue for any cutoff K [5]. This state is not displayed in the right panel of Figure 2.

Let us quote, for completeness, the continuum momentum limit of the eigen-equations of H_C which was used to obtain the $1/K = 0$ points in Fig. 2. They can be readily derived from the discretized matrix elements (27-32) or, equivalently, by applying our H_C (12,13) to the n-parton state and using rules of the planar calculus [22]. For two partons

---

[5]Many other massless states have been found in the literature [18] for any K . These are due to a finite-K artifact by which states with a large number of partons, $k \sim K$, are annihilated by the SUSY charges (and therefore by the Hamiltonian), since all transitions are blocked by the finite momentum resolution. Obviously only states with $k \ll K$ can be reliably computed in our approach.

one obtains:

$$E_C\varphi(p) = \frac{\lambda}{2\pi} \left[\int_\epsilon^p dq \frac{\varphi(p) - \varphi(p-q)}{q^2} + \int_\epsilon^{K-p} dq \frac{\varphi(p) - \varphi(p+q)}{q^2} \right] , \qquad (33)$$

which indeed is equivalent to 't Hooft equation:

$$E_C\varphi(x) = \frac{\lambda}{2\pi} PV \int_0^1 dy \frac{\varphi(x) - \varphi(y)}{(x-y)^2} . \qquad (34)$$

It is perhaps worth observing that in the former variables, i.e. in terms of the momentum transfer q, the linear *and* logarithmic divergencies clearly cancel leaving behind the finite right hand side of (33). This provides the justification for the principal value prescription commonly used in (34).

The multiparton generalizations follow from (12,13) as well

$$E\varphi(p_1, \dots p_n) =$$
$$\frac{\lambda}{2\pi} \sum_{i=1}^n \int_{-p_{i+1}+\epsilon}^{p_i-\epsilon} dq \frac{\varphi(p_1, \dots p_i, p_{i+1}, \dots p_n) - \varphi(p_1, \dots p_i - q, p_{i+1} + q, \dots p_n)}{q^2} , \qquad (35)$$

and, again, can be written in many equivalent forms [23].

6.2 Spatial structure of multiparton states

It turns out that the eigenstates of H_C have a very simple and natural structure which shows up most beautifully in position space. For $p = 2$ it is summarized in Fig. 3 where a sample of two parton eigenstates spanning the whole interval of eigenenergies is displayed. What is actually shown is the modulus squared of the discretized version of the Fourier transform

$$\psi_r(\Delta_{12}) = \int_0^P e^{-i\Delta_{12}p_1} \psi_r(p_1, P - p_1) dp_1, \qquad (36)$$

as a function of the relative, light cone, distance $\Delta_{12} = x_1 - x_2$, with ψ_r being the r-th eigenstate of (27). Upon the discretization all momenta and coordinates become dimensionless integers: $P \to K$, $p_1 \to m$, $\Delta_{12} \to d_{12}$.

The interpretation of the above Figure is clear. The eigenstates are very well localized in relative distance, and there is a very strong (linear in fact) correlation between d_{12} and r. In the lowest state two partons sit on top of each other and their energy is exactly zero. Excited states correspond to partons separated by a finite distance which gradually increases with the energy. Finally, in the highest state partons are maximally separated, i.e. are located at the antipodes of the circle (the Figure refers to $K = 201$). The relation between d_{12} and eigenenergy turns out to be linear, as expected in the one dimensional world (c.f. Sect.6.4). This also explains the linearity of the $p = 2$ plot in Fig. 1.
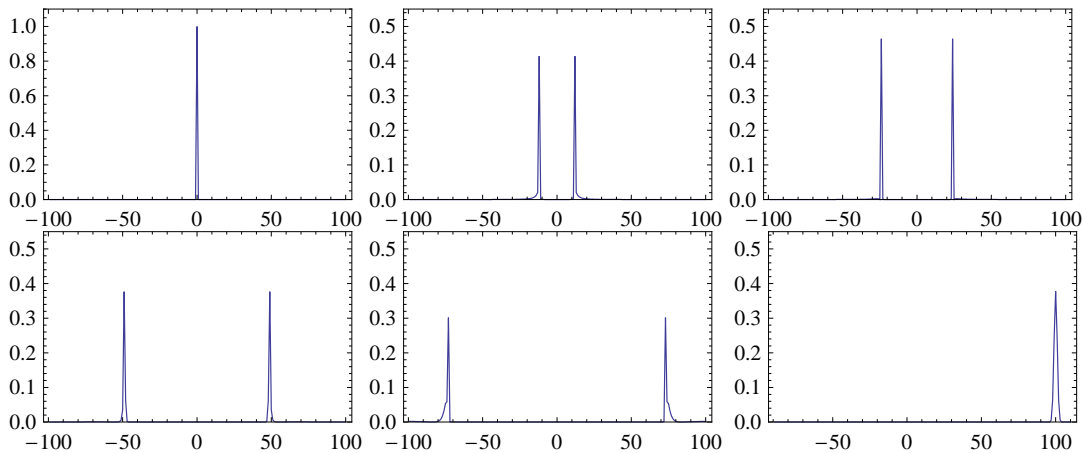
15

Figure 3: Space profiles of various eigenstates (36) with two partons, K=201 ($r = 1, 26, 50, 100, 150, 200$).

Interestingly, this picture generalizes naturally to many parton sectors. Figure 4 displays a sweep through three parton eigenstates obtained by diagonalization of (30). Coordinate space wave functions depend now on two independent relative distances which we choose as $\Delta_{13} = x_1 - x_3$ and $\Delta_{23} = x_2 - x_3$.

$$\psi_r(\Delta_{13}, \Delta_{23}) = \int_{p_1,p_2,p_3>0}^{P} e^{i\Delta_{13}p_1} e^{i\Delta_{23}p_2} \psi_r(p_1, p_2, P - p_1 - p_2) dp_1 dp_2 \,. \qquad (37)$$

Again, after the discretization the relative distances become integer: $1 \leq d_{13}, d_{23} \leq K-2$, with $K - 2$ being the period of the discrete Fourier transforms.

Similarly to the $p = 2$ case the wave functions are composed of a series of very narrow (in lattice units) structures which give a sharp localization in relative distances. Again the energy of the lowest state is exactly zero with all three partons located at the same point (upper left panel). Going to higher and higher states partons are moving apart migrating into the whole circle and finally, in the highest state, three partons are sitting at the maximal and equal distances forming the familiar "mercedes" star (lower right).

Obviously the structure of three parton states is much richer than that in the $p = 2$ sector. Nevertheless a number of regularities can be found which provide a compelling overall picture. They are better seen in the contour plots which we will now discuss.

Apparently the whole spectrum consists of a series of states with similar properties. Beginning of one such series is shown in Fig.5. Again we see that the higher the energy, the

16

larger are the inter-parton distances. The new feature is that now there are many peaks (i.e. parton configurations) in a single state. Part of it comes from the $\mathbb{Z}_3$ symmetry of the displayed densities. However the rest provides a beautiful confirmation of the linearity of the Coulomb potential and/or the underlying string picture. Namely, all parton configurations, composing a particular state in one series, appear to have the same value of the "combined string length" $l = |d_{12}| + |d_{23}| + |d_{31}|$. And vice versa: configurations with different l belong to states with different energy. As an illustration consider the fifth state displayed in Fig. 5. It has $l = 12$, this can be achieved, e.g. with partons 1 and 2 separated by 6 units and with parton no. 3 somewhere between the two. This is represented by 5 configurations (peaks) extending from $(d_{13}, d_{23}) = (1, -5)$ to $(5, -1)$ as no. 3 moves from no. 1 to no. 2. Similarly one can decode all structures appearing in that Figure. One more example: a horizontal ridge extending between $(-5, -6)$ and $(-1, -6)$, in that panel, describes partons 2 and 3 separated by 6 units and parton 1 located in five positions between the two.
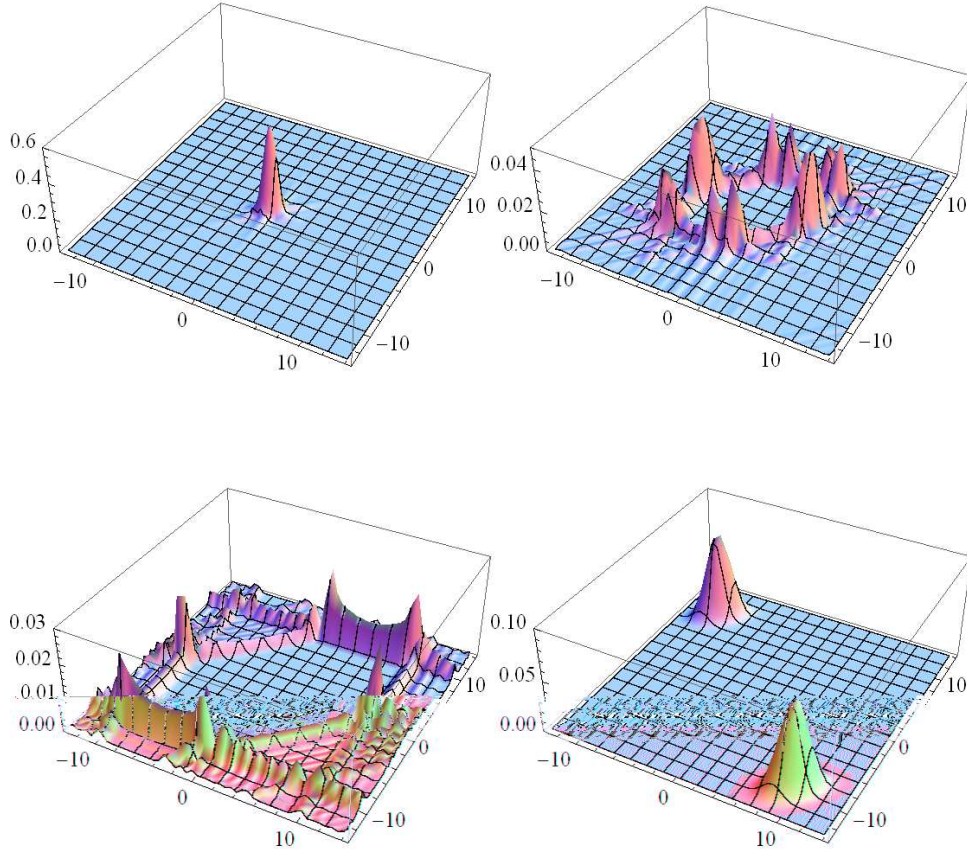
Figure 4: As in Fig.3, but for three partons and in terms of two relative distances d_{13} and d_{23}, $r = 1, 80, 120, 406$, $K = 30$.
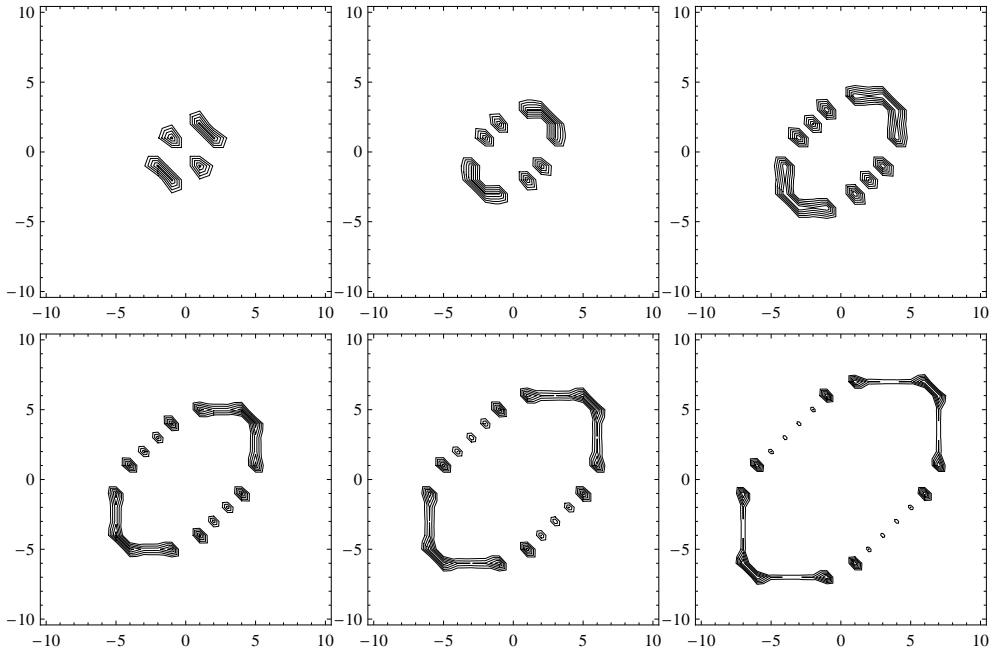
Figure 5: A clean series (A) of three parton eigenstates, $K = 100, \quad 4 \le l \le 14$.

The $\mathbb{Z}_3$ symmetry of planar states is not evident in these figures, because of the asymmetric variables used. However it is there and corresponds to $(x, y) = (d_{13}, d_{23}) \rightarrow (y - x, -x) \rightarrow (-y, x - y)$. The $\mathbb{Z}_3$ symmetric representation is shown in Fig.6 where another series is displayed on the massless "Dalitz plot" ensuring the constraint $d_{12} + d_{23} + d_{31} = 0$.

Finally, let us comment on the existence of different series in the many body spectrum which we find quite intriguing. As already said, we see "experimentally" that our three parton states group naturally into series. States in one series differ only by the increase of the relative distance between partons, as in Fig.5. However states from various series exhibit other differences. An example of another series was just given in Fig.6. Here again, increasing the inter parton distances increases the eigenenergy, however the pattern of the configuration remains the same. On the other hand, apart from the change of a display, there is a clear difference between patterns shown in Figures 5 and 6. In the first series (A) the partons never coincide, while in the other one (D) in every configuration one relative distance vanishes. However, we have also found other series where the differences are not so clear. In general, states from different series can have the same combined string length l and yet they have different energies. This suggests the existence of other conserved quantities, hence quantum numbers, which also control multiparton spectra.

Solutions in the four parton sector show qualitatively the same phenomena. In Fig 7 we display contour plots, in three relative distances d_{14}, d_{24} and d_{34}, of various eigenstates of (32). Again, in the lowest state all relative distances vanish; then, in higher states, partons gradually separate and in the highest state they group in two closely bound pairs sitting
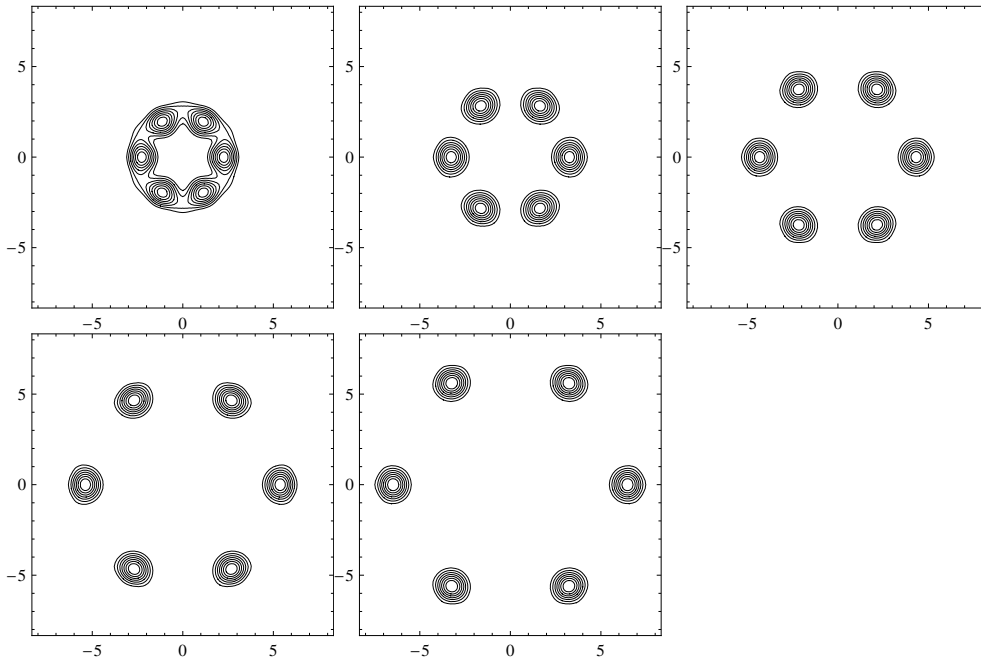
18

Figure 6: Different series (D) and on the "Dalitz plot".

at the antipodal locations on the circle. This is different than the naive extrapolation from the three parton case and illustrates how rich is the system with possibly more surprises at higher multiplicities. Similarly to $p = 2, 3$, states are sharply localized in the relative distances and separations between various partons can be determined.

Obviously, multidimensional representations like Fig.7 become unpractical for higher multiplicities. An alternative way to proceed is to study inclusive densities and correlations. In our case, e.g. in a given p parton sector, an inclusive single parton density can be defined as

$$D_r(\Delta) = \int d^{p-1}\vec{\Delta}_p \sum_{i=1}^{p-1} \delta(\Delta - \Delta_{in})|\psi_r(\vec{\Delta}_p)|^2 \tag{38}$$

and gives the number of partons at a distance Δ from i.e. the last one. It can be easily calculated from our exclusive wave functions or, yet simpler, directly from the Fourier components. The latter representation reads, e.g. in the four parton case,

$$D_r(\Delta) = \int_{p_2,p_3,P-p_2-p_3>0}^{P} dp_2 dp_3 |\psi_r(\Delta, p_2, p_3)|^2 + cycl. \tag{39}$$

with $\psi_r(\Delta, p_2, p_3)$ standing for the partial Fourier transform - only in the first variable.

In Fig. 8 above density is shown in the four parton sector. It confirms what we have already learned from the exclusive data. However the structure of four parton states can now be seen in more detail. Rather than sweeping through the whole spectrum, we
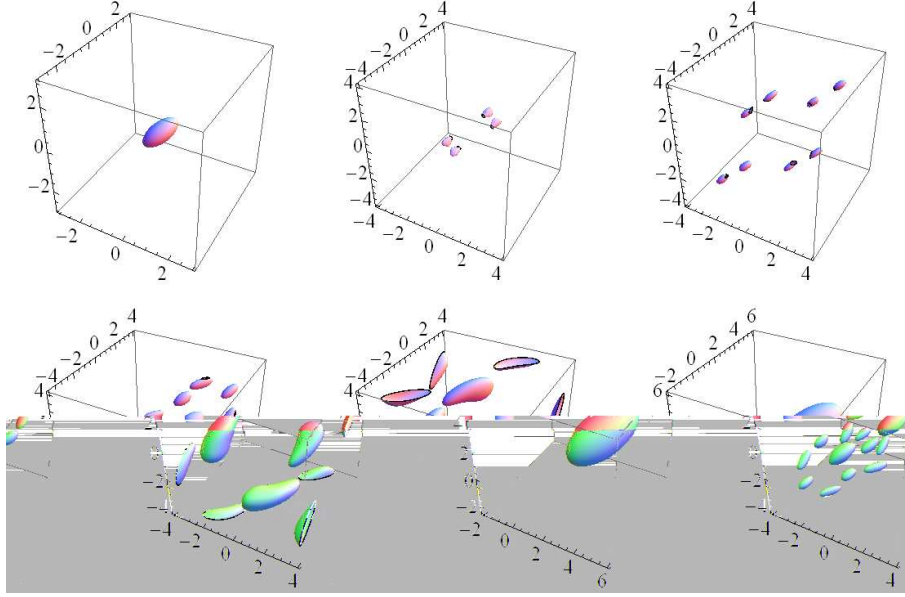
19

Figure 7: Structure of eigenstates with four partons. Contour plots in three relative distances (d_{14}, d_{24}, d_{34}) for states no. 1,9,35,60,100,165 spanning the whole range of states for $K = 12$, $r_{max} = 165$.

have concentrated on lower states. Fig.8 clearly shows the growth of the distance between the two outermost partons and how the intermediate positions between the two are populated. Of course the complete information could be recovered only upon examining simultaneously higher inclusive densities.

6.3 Some analytic considerations

Let us now discuss some analytic aspects of the solutions. To this date such solutions are not available in spite of many attempts [24]. Generalization for many bodies only increases the challenge. We believe however that the numerical studies presented here can also contribute to the analytic understanding of these systems. Consider for example the massless, $E_C = 0$, bound state. It has been found numerically, and it is obvious from (35) that such a solution exists for all multiplicities and has a constant wave function in the momentum representation. It is then a simple matter to construct its (LC) configuration space counterpart. For two partons we have

$$\psi(x_1, x_2) = c \int_0^P dp_1 dp_2 e^{-ix_1 p_1 - ix_2 p_2} \delta(p_1 + p_2 - P)$$
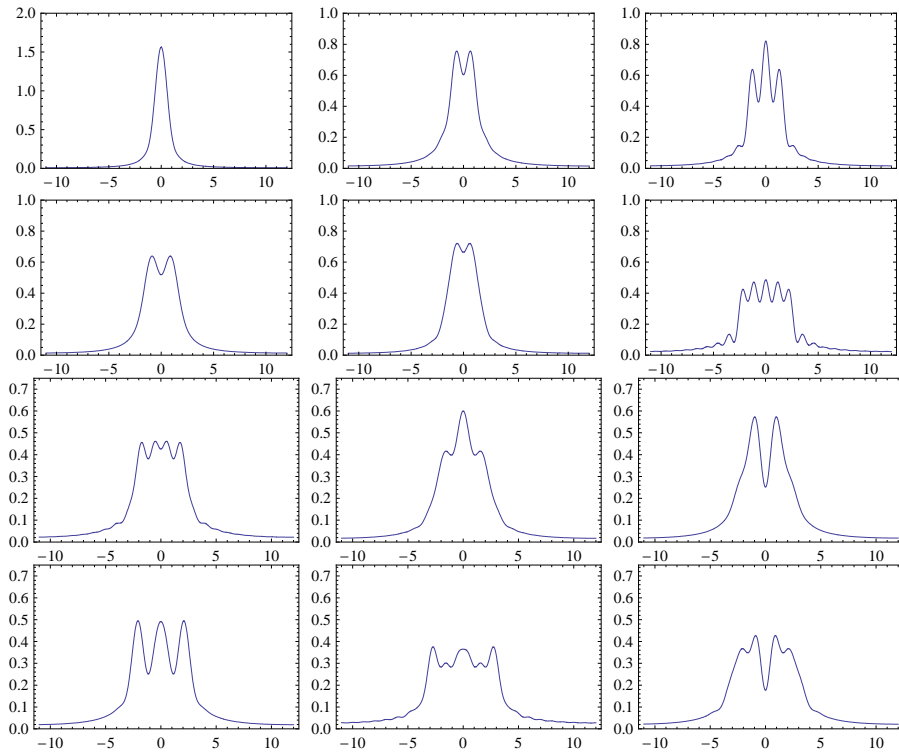$$= e^{-iP(x_1+x_2)/2} \frac{\sin(P\Delta_{12})}{\sqrt{P}\Delta_{12}}, \tag{40}$$

Figure 8: Inclusive single parton density for four partons and for lower states $r = 1, 4, 5, 6, 9, 12, 13, 14, 15, 20, 26, 29$, $K = 27$, $r_{max} = 2600$.

with the (not normalized) probability distribution depending only on Δ_{12}

$$|\psi|^2 = \frac{\sin^2(P\Delta_{12})}{P\Delta_{12}^2} \, . \tag{41}$$

For three partons one obtains analogously

$$\psi(x_1, x_2, x_3) = c \int_0^P dp_1 dp_2 dp_3 \; \delta(p_1 + p_2 + p_3 - P) e^{-ip_1 x_1 - ip_2 x_2 - ip_3 x_3} =$$

$$= ic \frac{e^{-ix_3 P}}{2\Delta_1 \Delta_2 (\Delta_1 - \Delta_2)} \left(\Delta_1 e^{-i\Delta_2 P} \sin(\Delta_2 P) - \Delta_2 e^{-iP\Delta_1} \sin(\Delta_1 P) \right) \, , \tag{42}$$

where we used $\Delta_1 = \Delta_{13}/2, \Delta_2 = \Delta_{23}/2$ as relative distances. Upon normalization $c = P/\sqrt{2}$, we obtain for the density

$$|\psi|^2 = \frac{P^2}{32\Delta_1^2 \Delta_2^2 (\Delta_1 - \Delta_2)^2} \left[(\Delta_1 \sin(2\Delta_2 P) - \Delta_2 \sin(2\Delta_1 P))^2 + \right.$$

$$\left. + 4(\Delta_1 \sin^2(\Delta_2 P) - \Delta_2 \sin^2(\Delta_1 P))^2 \right] \, , \tag{43}$$

which is completely symmetric in exchanging Δ_1 with Δ_2 and regular for $\Delta_1, \Delta_2 \to 0$. As for the two parton case we see that in the limit $P \to \infty$ we find a δ-function centered at zero, both for Δ_1 and Δ_2, confirming that actually the zero energy state corresponds to three partons sitting all together at the same position.

Generalizing this computation to higher sectors is trivial, hence the massless eigenstates can be constructed analytically in all multiplicity sectors.

6.4   String picture

The findings reported so far support the widely accepted string picture of (1+1)- dimensional planar gauge theories. The relation is quite natural, even hardly surprising, in the case of two partons. It is also generally expected with more partons, however our results provide a direct illustration of how this is happening.

We have seen that the two parton eigenstates are very well localized in (LC) configuration space. Consequently, the length of the effective string between two partons can be readily extracted from our eigenstates (c.f. Fig.3). Figure 9 shows the dependence of the eigenenergies on that length. It approaches a nice linear form at large cutoff, K, with a well defined, finite, string tension.

There is an interesting correlation between the parity under the reflection $k \leftrightarrow P - k$, and the inter parton distances. Namely, in even (odd) states partons are separated by integer (half-integer) distances. This explains why the eigenenergies of the symmetric and antisymmetric states are half a way between each other in Fig. 2

Before moving to higher multiplicities, let us compare our numerical results with the theoretical prediction for the effective string tension in the two-parton case, $\sigma = \lambda/2$ [20, 21]. Fig.10 shows the ratio of two parton eigenenergies to the combined string length
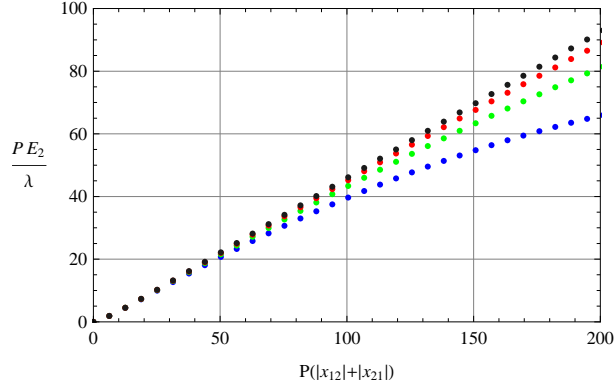
Figure 9: Two-parton energies, as a function of (doubled) parton separation, for increasing K. Different colors (bottom to top) correspond to $K = 50, 100, 200, 400$.
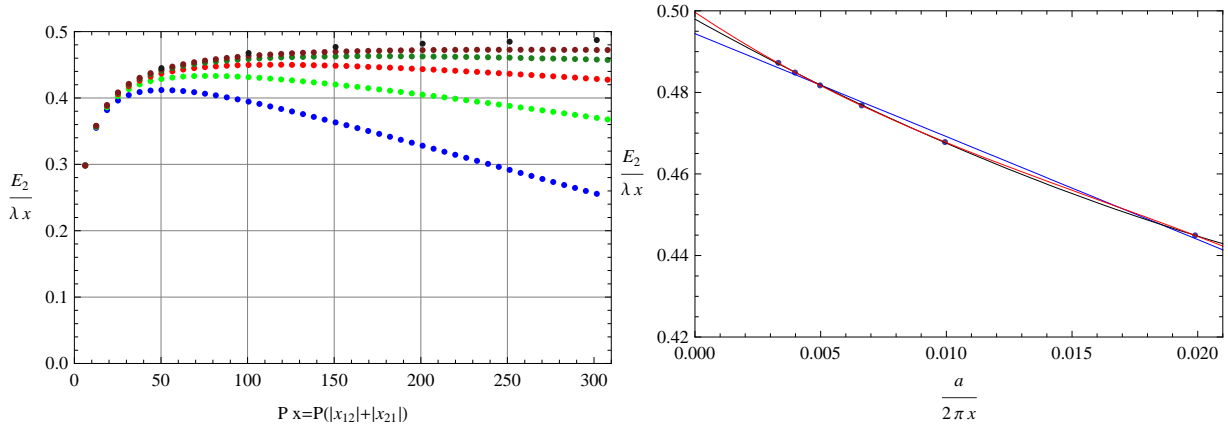

Figure 10: Left: as in Fig.9 but for the string tension together with the extrapolations to $K = \infty$ (black). Right: polynomial extrapolations (see the text) to $a = 0$.

$x = |x_{12}| + |x_{21}|$, in units of λ, as a function of the dimensionless lattice distance $Px = 2\pi x/a = 2\pi l$. Different colors show results for different cutoffs, $K = 50, 100, 200, 400, 800$.

As expected, there is a significant cutoff dependence for larger parton separations. The K dependence is however rather weak and can be easily taken care of. Black points show results of the polynomial (in $1/K$) extrapolation to $K = \infty$, at few values of l. In lattice terminology they correspond to the string tension determined from finite lattice distances hence are still biased by finite a effects. To get rid of the latter one has to perform the continuum (i.e. $a \to 0$) limit. This is summarized in Fig.10 where the a/x dependence of above K extrapolations is displayed. Again the a/x dependence is mild and polynomial fits provide quite stable extrapolations to $a = 0$. Those are in very satisfactory agreement with the theory cf. Table I.

With three partons, situation is yet more interesting. Assigning automatically the combined string length l to each state on the basis of integer coordinates of sharp peaks

M	1	2	3
$W_M(0)$	0.4944	0.4980	0.4997

Table 1: First three polynomial extrapolations of the a dependence of the string tension from Fig.10.
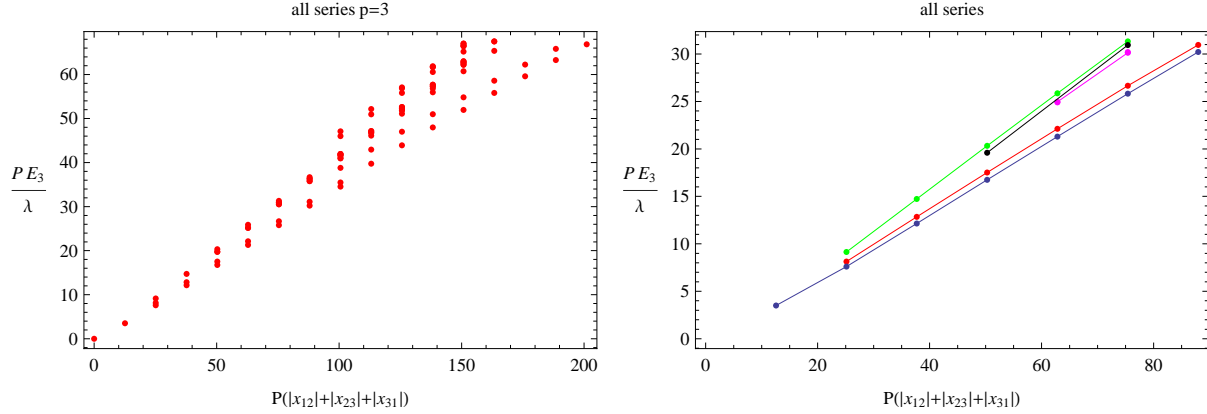

Figure 11: Eigenenergies of three parton states vs. the combined string length l.

in the density, results in Fig. 11 (left, $K = 100$). This only confirms the existence of some ambiguities. We have already found, however, that there are series of states composed of similar patterns of configurations. Could they account for what is seen in Fig. 11? In fact yes, in the right panel of Fig. 11 we show similar plot but constructed for five series identified by inspection of lowest 20 eigenstates. Two of them were described in the previous subsection. Indeed, for each series we observe a clean linear growth of the energy with l. The slope of that dependence is consistent (albeit somewhat smaller) with the one seen for two partons.
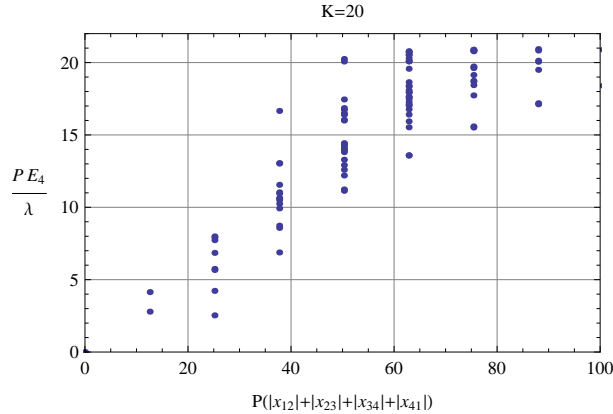

Figure 12: As in Fig.11 but for four partons.

Similar behaviour is seen in the four parton sector, Fig. 12, obviously the situation is

more complex with more families and larger spread of energies at fixed "l". No attempt was made to identify separate series yet and to extract the string tension. The latter requires the former and extrapolations in K and a, as was done for $p = 2$.

Clearly more detailed studies are needed to unravel a complete structure of higher parton states. In particular comparison with the direct solutions of 't Hooft equations in higher-p sectors would be very useful.

6.5   Pre-SUSY

As already mentioned our drastic approximation breaks half of the original supersymmetry leaving behind just the $\mathcal{N}(1,1)$ subgroup generated by Q_2, $Q_2^\dagger$. In spite of this it is amusing to compare the spectra of sectors that should be connected by the action of all the SUSY charges. The supersymmetry generated by Q_2, $\bar{Q}_2$ connects states with the same number of partons and is self-evident in our graphs. On top, there are further degeneracies between states with the same p due to our Coulomb approximation. It is clear, instead, that there is no exact degeneracy for states of different p even if some of them should be connected through the action of the Q_1, $\bar{Q}_1$ generators.
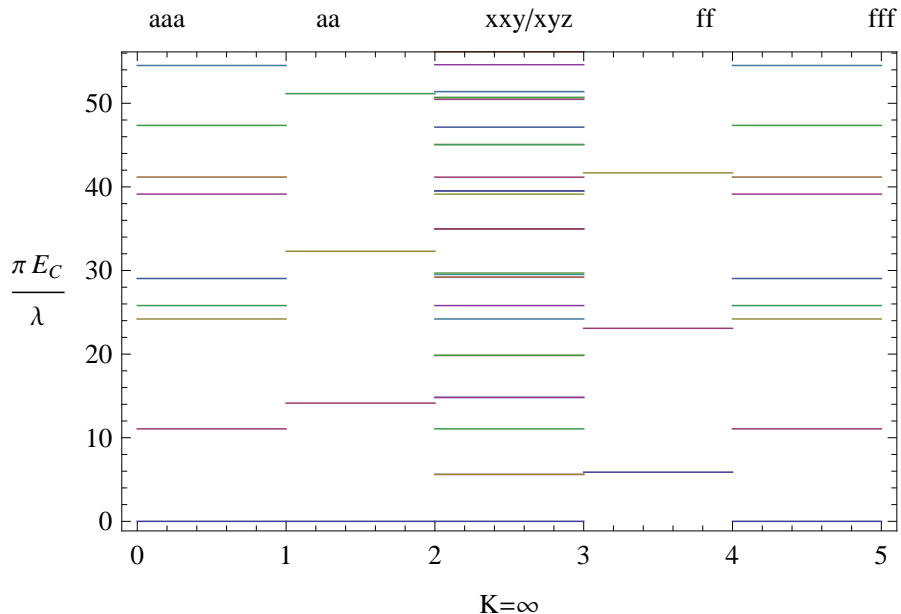

Figure 13: The lowest levels with 2 and 3 partons. Here a represents either a or b and f either f or g. For $p = 2$ the aa and ff spectra, for identical partons, are complementary and their sum gives all the unequal-parton spectra. For $p = 3$ the xxx (i.e. aaa or fff) spectra are all identical but contain far less states than the xxy or xyz spectra. The xyz spectra are equal to the xxy spectra modulo a doubling of the states since xyz and xzy are two distinct, but degenerate, states.

Let us consider, as an example, the Konishi (anomaly) supermultiplet keeping Fig. 13

in mind. As discussed in section 2.1 the full chiral supemultiplet in this case contains $p = 2$ states of non-identical partons and $p = 3$ states in which there are at least two different species. The corresponding energy levels match the union of the aa and ff spectra in the figure and the central (xxy/xyz) levels. We see that there is (decreasingly) good matching for the first three excited levels while for the fourth the matching is already quite poor (for higher levels the good matching looks a bit accidental given the high density of $p = 3$ levels).

Consider now a different supermultiplet, one that contains the state $|aa\rangle$. Its partners should be found in the af sector and in the aaf and aff sectors and all works as in the previous case.

Consider finally the supermultiplet containing the state $|ff\rangle$. Apparently we find a problem since the lowest excited ff state has no nearly-degenerate partner in the fff sector. However this is as it should be: the $|ff\rangle$ wavefunction must be odd under the interchange of the two momenta. When one applies Q_1 to it one finds that this antisymmetry clashes with the symmetry needed in $|fff\rangle$. Instead, the $|ff\rangle$ state should form a multiplet with $|af\rangle$, $|afg\rangle$ and $|abf\rangle$. The matching is now excellent.

In conclusion, although a priori our drastic truncation of the Hamiltonian could have left no sign at all of the supersymmetry generated by Q_1 and $\bar{Q}_1$, we have found that some trace of the full $\mathcal{N} = (2, 2)$ supersymmetry appears to have survived in the spectra of H_C. This makes us confident that our truncated Hamiltonian may represent a fairly good approximation to the exact one.

7   Conclusions and outlook

We have considered the dimensional reduction of $D = 4$, $\mathcal{N} = 1$ SYM theory to two dimensions in the large-N (planar) limit using the LC gauge and LC quantization. This allows us to explicitly eliminate all non-physical degrees of freedom at the price of having a non-local LC Hamiltonian. Nonetheless, such an Hamiltonian exhibits many desirable features: it is invariant under $\mathcal{N} = (2, 2)$ supersymmetry transformations provided these are suitably defined in order not to destroy the LC-gauge choice; it is manifestly normal-ordered and positive-semidefinite so that it possesses an exact zero-energy ground state and a spectrum of non-negative energy excitations.

In order to solve for the eigenvalues and eigenstate of the Hamiltonian we have compactified LC-space to a circle of radius R allowing to work within a finite Hilbert space as long as we keep the conserved LC momentum of our states finite, the idea being, of course, to eventually send R to infinity and check that physical quantities approach a finite smooth limit.

Infrared (IR) divergences appear to make this task somewhat technically complicated (although in principle possible) and therefore, in this first paper, we have truncated the Hamiltonian to what looks superficially as its most IR divergent part. Indeed, for the colour-singlet, single-trace states that survive in the large-N limit, these linear IR divergences are neatly cancelled and get replaced by an effective Coulomb interaction

which, in $D = 2$ gives a confining linear potential. We have then studied many properties of the eigenvalues and eigenfunctions of this Coulomb Hamiltonian, H_C, and confirmed that, at least in this approximation, the large R limit is smooth (although larger and larger R are needed before heavier and heavier states stabilize).

The resulting model breaks supersymmetry down to an $\mathcal{N} = (1,1)$ subgroup and looks like a supersymmetric generalization of 't Hooft's original model [15] where states with an arbitrary number of partons are present even at leading order in $1/N$.

When seen in position-space a nice string picture emerges in which the mass of each state is proportional to the sum of the (center-of-mass distances) of each pair of neighbouring partons. These distances are quite sharply quantized leading to a discrete spectrum with approximately linear "Regge" trajectories. The numerical value of the proportionality constant (the string tension) agrees very well with theoretical expectations. For states with more than two partons the situation is obviously richer. Yet we were able to identify clean series of three-parton states whose eigenenergies are indeed proportional to the combined length of strings stretched between neighbouring partons. Moreover, the detailed patterns of parton configurations contributing to these states confirm unambiguously the linear form of the two-body interactions. String tension seen in these sectors is compatible with the one extracted from the two parton sector.

In our Coulomb approximation the first excitation over the Fock vacuum is also massless with all the partons sitting at the same point but this is most likely an artifact of our Coulomb approximation that allows all partons to sit at the same point without paying any kinetic-energy price. Since even those massless states are nicely paired in supermultiplets, we expect them to be lifted to some finite energy. Indeed, if we add some finite terms present in the full Hamiltonian (5), we see that these state acquire a non-zero energy. At least in our approximation we find no evidence (apart from the just mentioned states) for the absence of a mass gap reported in some previous studies [18]. We also see clearly how the existence of many other massless states, for each value of R, is nothing but a consequence of the breakdown of the method when the number of partons approaches its maximal value compatible with momentum conservation.

Finally, we found that, even in our drastic approximation the full $\mathcal{N} = (2,2)$ supersymmetry of the original model shows up as an approximate supermultiplet structure at least for the lightest states. Our belief is that the "worst" divergent part in (5) gives us the bulk structure of the energy states, namely the nice discrete linear spectrum. We expect the logarithmic IR singularities to lead to a dressing of our states à la Block-Nordsieck and to modify the energies by lifting, in particular, the zero-energy states. We plan to report on progress in this direction in a forthcoming paper.

Acknowledgements

Note Added

After having circulated a preliminary version of this paper we became aware of previous work [25], [26], [27], [28], claiming that two-dimensional theories of the kind we considered (i.e. with massless fermions in the adjoint representation) should exhibit a Schwinger-like phenomenon even in the planar large-N limit. This would result in the screening of the linear potential and in the spectrum becoming continuous above a certain energy scale. If this were true, it would mean that the terms we neglected should have a dramatic effect, at least for the high-energy part of the spectrum. This point, as well as the dependence of the spectrum itself on the scalar VEV, clearly deserve further investigations. We are grateful to A. Armoni for bringing the abovementioned papers to our attention.

References

[1] G. 't Hooft, "A planar diagram theory for strong interactions," *Nucl. Phys.*, vol. B72, p. 461, 1974.

[2] G. Veneziano, "Some Aspects of a Unified Approach to Gauge, Dual and Gribov Theories," *Nucl. Phys.*, vol. B117, pp. 519–545, 1976.

[3] J. M. Maldacena, "The large N limit of superconformal field theories and supergravity," *Adv. Theor. Math. Phys.*, vol. 2, pp. 231–252, 1998.

[4] E. Witten, "Anti-de Sitter space and holography," *Adv. Theor. Math. Phys.*, vol. 2, pp. 253–291, 1998.

[5] A. Armoni, M. Shifman, and G. Veneziano, "Exact results in non-supersymmetric large N orientifold field theories," *Nucl. Phys.*, vol. B667, pp. 170–182, 2003.

[6] A. Armoni, M. Shifman, and G. Veneziano, "SUSY relics in one-flavor QCD from a new 1/N expansion," *Phys. Rev. Lett.*, vol. 91, p. 191601, 2003.

[7] A. Armoni, M. Shifman, and G. Veneziano, "QCD quark condensate from SUSY and the orientifold large-N expansion," *Phys. Lett.*, vol. B579, pp. 384–390, 2004.

[8] A. Armoni, G. Shore, and G. Veneziano, "Quark condensate in massless QCD from planar equivalence," *Nucl. Phys.*, vol. B740, pp. 23–35, 2006.

[9] M. Unsal and L. G. Yaffe, "Large-N volume independence in conformal and confining gauge theories," *JHEP*, vol. 08, p. 030, 2010.

[10] P. Kovtun, M. Unsal, and L. G. Yaffe, "Volume independence in large N(c) QCD-like gauge theories," *JHEP*, vol. 06, p. 019, 2007.

[11] M. Unsal and L. G. Yaffe, "Center-stabilized Yang-Mills theory: confinement and large N volume independence," *Phys. Rev.*, vol. D78, p. 065035, 2008.

[12] T. Eguchi and H. Kawai, "Reduction of Dynamical Degrees of Freedom in the Large N Gauge Theory," *Phys. Rev. Lett.*, vol. 48, p. 1063, 1982.

[13] S. J. Brodsky, H.-C. Pauli, and S. S. Pinsky, "Quantum Chromodynamics and Other Field Theories on the Light Cone," *Phys. Rept.*, vol. 301, pp. 299–486, 1998.

[14] A. Armoni and J. Sonnenschein, "Mesonic spectra of bosonized QCD in two-dimensions models," *Nucl. Phys.*, vol. B457, pp. 81–95, 1995.

[15] G. 't Hooft, "A Two-Dimensional Model for Mesons," *Nucl. Phys.*, vol. B75, p. 461, 1974.

[16] Y. Matsumura, N. Sakai, and T. Sakai, "Mass spectra of supersymmetric Yang-Mills theories in (1+1)-dimensions," *Phys. Rev.*, vol. D52, pp. 2446–2461, 1995.

[17] J. Terning, "Modern supersymmetry: Dynamics and duality," Oxford University Press, Oxford, UK (2006).

[18] M. Harada, J. R. Hiller, S. Pinsky, and N. Salwen, "Improved results for N = (2,2) super Yang-Mills theory using supersymmetric discrete light-cone quantization," *Phys. Rev.*, vol. D70, p. 045015, 2004.

[19] P. C. West, "Introduction to supersymmetry and supergravity," World Scientific Publishing Company, Singapore (1990).

[20] V. A. Kazakov and I. K. Kostov, "Nonlinear strings in two-dimensional $U(\infty)$ gauge theory," *Nucl. Phys.*, vol. B176, pp. 199–215, 1980.

[21] V. A. Kazakov, "Wilson loop average for an arbitrary contour in two-dimensional $U(N)$ gauge theory," *Nucl. Phys.*, vol. B179, pp. 283–293, 1981.

[22] G. Veneziano and J. Wosiek, "Planar quantum mechanics: An intriguing supersymmetric example," *JHEP*, vol. 01, p. 156, 2006.

[23] G. Bhanot, K. Demeterfi, and I. R. Klebanov, "(1+1)-dimensional large N QCD coupled to adjoint fermions," *Phys. Rev.*, vol. D48, pp. 4980–4990, 1993.

[24] V. A. Fateev, S. L. Lukyanov, and A. B. Zamolodchikov, "On mass spectrum in 't Hooft's 2D model of mesons," *J. Phys.*, vol. A42, p. 304012, 2009.

[25] D. J. Gross, I. R. Klebanov, A. V. Matytsin, and A. V. Smilga, "Screening vs. Confinement in 1+1 Dimensions," *Nucl. Phys.*, vol. B461, pp. 109–130, 1996.

[26] A. Armoni, Y. Frishman, and J. Sonnenschein, "The string tension in massive QCD(2)," *Phys. Rev. Lett.*, vol. 80, pp. 430–433, 1998.

[27] D. J. Gross, A. Hashimoto, and I. R. Klebanov, "The spectrum of a large N gauge theory near transition from confinement to screening," *Phys. Rev.*, vol. D57, pp. 6420–6428, 1998.

[28] A. Armoni, Y. Frishman, and J. Sonnenschein, "Screening in supersymmetric gauge theories in two dimensions," *Phys. Lett.*, vol. B449, pp. 76–80, 1999.